Linear viscoelasticity of rubber: background, measurement, creation of master curves, relation to finite element codes and check for physical consistency (version 0.5)

Jan Plagge[a]

[a]Bergische Universität Wuppertal, Gaußstr. 20, Wuppertal, D-42097, NRW, Germany

ABSTRACT

Linear viscoelasticity is a well established and well understood theory. However, there are still serious misconceptions around and people from different disciplines often use different ways of thinking and conventions to talk about the same subject. This article aims to give a compact overview about how to work with and understand linear viscoelasticity, how to measure dynamic moduli and how to convert them reliably to viscoelastic mastercurves. Finally, the relation to differential equations typically used in finite element analysis is shown and a relatively simple way to check for physical consistency (i.e. verifying Kramers-Kronig relations) is presented.

1. Introduction

...tbd ...

2. Theory

2.1. Basics of linear viscoelasticity

In *linear* viscoelasticity the stress response $\sigma(t)$ is fully defined by relaxation function $G(t)$ and strain rate $\dot{\varepsilon}$ as

$$\sigma(t) = \int_0^t G(t-t')\dot{\varepsilon}(t')\,\mathrm{d}t' \tag{1}$$

with this definition σ is a linear function of strain ε (the integral and derivative are linear operators). The corresponding integral is also called hereditary integral. Non-linear viscoelasticity is not treated in this article and we refer to Tolpekina, Pyckhout-Hintzen and Persson (2019) as a starting point. Two special cases may be instructive. If the relaxation function is constant in time, e.g. $G(t) = G_0\theta(t)$, we get

$$\sigma(t) = G_0 \int_0^t \theta(t-t')\dot{\varepsilon}(t')\,\mathrm{d}t' \tag{2}$$

$$= G_0 \int_0^t \dot{\varepsilon}(t')\,\mathrm{d}t' \tag{3}$$

$$= G_0\varepsilon \tag{4}$$

corresponding to a "Hooke's spring" with spring constant (modulus) G_0. The other extreme case is when $G(t)$ decreases "infinitely fast", i.e. it samples just the actual strain rate. This can be expressed by the Dirac delta distribution, viz. $G(t) = \eta_0\delta(t)$

$$\sigma(t) = \eta_0 \int_0^t \delta(t-t')\dot{\varepsilon}(t')\,\mathrm{d}t' = \eta_0\dot{\varepsilon}(t) \tag{5}$$

which is the well-known formula of a fluid or pure damper with damping coefficient η_0. Rubber is between both extrema and the relaxation function $G(t)$ fully determines its response at small strains (linear regime). In practice it can be measured in several ways.

One possibility is to stretch a sample as fast as possible to a defined strain ε_0, holding it a t this strain and watching the decay in stress $\sigma(t)$, see Figure 1c. The experiment can be formalized by

$$\varepsilon(t) = \varepsilon_0\theta(t) \tag{6}$$

$$\rightarrow \dot{\varepsilon}(t) = \varepsilon_0\delta(t) \tag{7}$$

where the θ-function "switches on" strain infinitely fast for $t > 0$. This gives

$$\sigma(t) = \varepsilon_0 \int_0^t G(t-t')\delta(t')\,\mathrm{d}t' = \varepsilon_0 G(t) \tag{8}$$

We see that $G(t)$ can be directly deduced from the decay of stress. However, this way is often impractical, because two effects restrict the reliable time interval of $G(t)$: Stretching speed of the machinery is limited, such that there may be relaxation during stretching (see dashed line in Figure 1c). This spoils the low t-regime (high frequency regime). On the other hand relaxation slows down at large t, so that changes in stress are too small to be detected. For these reasons a common procedure is to watch the response to a sinusoidal signal. At this point one can take advantage of the Convolution theorem of the Fourier transform. In fact, Eq. (1) can be restated as

$$\sigma(t) = \int_0^t G(t-t')\dot{\varepsilon}(t')\,\mathrm{d}t' \tag{9}$$

$$= \int_{-\infty}^{\infty} G(t-t')\dot{\varepsilon}(t')\,\mathrm{d}t' \tag{10}$$

$$= [G * \dot{\varepsilon}](t) \tag{11}$$

where the second equality exploits the fact that at some point in history the experiment has to start ($\dot{\varepsilon}(t \leq 0) = 0$) and causality ($G(t \leq 0) = 0$). The Convolution theorem

ORCID(s):

states that the Fourier transform of the convolution of two functions is the product of the Fourier transforms of both functions, so

$$\mathcal{F}[\sigma](\omega) := \hat{\sigma}(\omega) = \mathcal{F}[G * \dot{\varepsilon}](\omega) \tag{12}$$

$$= \sqrt{2\pi}\ \mathcal{F}[G](\omega) \cdot \mathcal{F}[\dot{\varepsilon}](\omega) \tag{13}$$

$$= \sqrt{2\pi}\ \hat{G}(\omega) \cdot (i\omega)\,\hat{\varepsilon}(\omega) \tag{14}$$

By simple rearrangement we get

$$G^*(\omega) := \frac{\hat{\sigma}(\omega)}{\hat{\varepsilon}(\omega)} = \sqrt{2\pi}\ i\omega\,\hat{G}(\omega) \tag{15}$$

where G^* is called dynamic modulus and is commonly measured using oscillatory strain on a rheometer, which allows to sample each frequency ω separately.
To see this, let us compute the response to a sinusoidal signal

$$\varepsilon(t) = \varepsilon_0 \cdot \sin(\Omega t) \tag{16}$$

$$\hat{\varepsilon}(\omega) = \varepsilon_0 \sqrt{2\pi} \frac{\delta(\omega - \Omega) - \delta(\omega + \Omega)}{2i} \tag{17}$$

where the Fourier transform follows directly from the Euler identity. δ is the Dirac Delta distribution function.
Starting from Eq. (15) the calculations are straightforward

$$\hat{\sigma}(\omega) = G^*(\omega)\hat{\varepsilon}(\omega) \tag{18}$$

$$= \sqrt{2\pi}\varepsilon_0\, G^*(\omega)\, \frac{\delta(\omega - \Omega) - \delta(\omega + \Omega)}{2i} \tag{19}$$

Transforming back into the time domain yields

$$\sigma(t) = \frac{1}{\sqrt{2\pi}} \int_{-\infty}^{\infty} \mathrm{e}^{i\omega t} \hat{\sigma}(\omega)\, \mathrm{d}\omega \tag{20}$$

$$= \varepsilon_0 \int_{-\infty}^{\infty} \mathrm{e}^{i\omega t}\, G^*(\omega)\, \frac{\delta(\omega - \Omega) - \delta(\omega + \Omega)}{2i}\, \mathrm{d}\omega \tag{21}$$

$$= \varepsilon_0 \left(\frac{\mathrm{e}^{i\Omega t}}{2i}\, G^*(\Omega) - \frac{\mathrm{e}^{-i\Omega t}}{2i}\, G^*(-\Omega) \right) \tag{22}$$

In the time domain G^* is a real valued function, such that for its Fourier transform $G^*(\Omega) = \bar{G}^*(-\Omega)$ holds, where the top bar denotes the complex conjugate. Splitting G^* into its real and imaginary part $G^* = G' + iG''$ we get

$$\sigma(t) = \sqrt{2\pi}\varepsilon_0 \left(\frac{\mathrm{e}^{i\Omega t}}{2i} (G' + iG'') - \frac{\mathrm{e}^{-i\Omega t}}{2i} (G' - iG'') \right) \tag{23}$$

$$= \varepsilon_0 \left(G' \frac{\mathrm{e}^{i\Omega t} - \mathrm{e}^{-i\Omega t}}{2i} + G'' \frac{\mathrm{e}^{i\Omega t} + \mathrm{e}^{-i\Omega t}}{2} \right) \tag{24}$$

$$= \varepsilon_0 \left(G'(\Omega) \sin(\Omega t) + G''(\Omega) \cos(\Omega t) \right) \tag{25}$$

Thus, oscillatory rheological measurements allow to sample each frequency of the Fourier transform of the relaxation function, see Figure 1a and b. Measuring the latter in the frequency- or time domain is mathematically fully equivalent (it Eq. (15) is taken into account). However, oscillatory measurements can be very easily combined with the *time-temperature superposition principle*, see below.

2.2. Practical evaluation of rheometer data

An idealized sketch of rheometer data is presented in Figure 1a (top). If a sine-strain according to Eq. (16) is employed a linear viscoelastic material will respond with a sine as well, but phase shifted by an angle δ. Using the trigonometric identity $a\sin(\alpha) + b\cos(\alpha) = \sqrt{a^2 + b^2}\sin(\alpha + \arctan(b/a))$ we transform Eq. (25) into

$$\sigma(t) = \varepsilon_0 |G^*| \sin(\Omega t + \delta) \tag{26}$$

$$|G^*| = \sqrt{G'^2 + G''^2} \tag{27}$$

$$\delta = \arctan\left(\frac{G''}{G'}\right) \tag{28}$$

where the moduli and δ generally depend on Ω as well. Thus, by plotting stress and strain according to Figure 1a (top) and determining peak stress $\varepsilon_0|G^*|$ as well as phase shift δ we can determine storage and loss modulus according to

$$G' = |G^*| \cos(\delta) \tag{29}$$

$$G'' = |G^*| \sin(\delta) \tag{30}$$

Alternatively, one may plot σ vs. ε for one (stable) cycle according to Figure 1a (bottom). For ideally viscoelastic materials this will always be an ellipse, and a deviation of this shape indicates some kind of non-linearity. In this representation, the elastic modulus can be determined by a fit of a linear function (line). Fitting is usually performed by minimizing the squared distance of data and function. The latter is also called error functional Err and can, in our case, be represented as an integral over the deformation cycle

$$Err = \int_0^{2\pi/\Omega} (\sigma(t) - m\,\varepsilon(t))^2\, \mathrm{d}t \tag{31}$$

$$= \frac{\pi}{\Omega} \left((m - G')^2 + G''^2 \right) \tag{32}$$

where $m\,\varepsilon(t)$ parameterizes a line through the origin with slope m, which is our quantity of interest. In the second step Eqs. (25) and (16) were inserted. Minimization with respect to m generates

$$\frac{\mathrm{d}Err}{\mathrm{d}m} = \frac{2\pi}{\Omega}(m - G') = 0 \ \Rightarrow\ G' = m \tag{33}$$

which shows us that, for linear viscoelastic materials, the slope of a line through the origin equals the storage modulus. As the area under the $\varepsilon - \sigma$-curve is the dissipated energy W_d, it is not surprising that it is directly related to the loss modulus. We thus write

$$W_d = \int_C \sigma\, \mathrm{d}\varepsilon = \int_0^{2\pi/\Omega} \sigma(t)\, \dot{\varepsilon}(t)\, \mathrm{d}t = \pi\, \varepsilon_0^2\, G'' \tag{34}$$

where we inserted, again, Eqs. (25) and (16). We thus arrive at

$$G'' = \frac{W_d}{\pi\, \varepsilon_0^2} \tag{35}$$

It depends on personal choice and probably technical resolution which of the two methods is preferred.

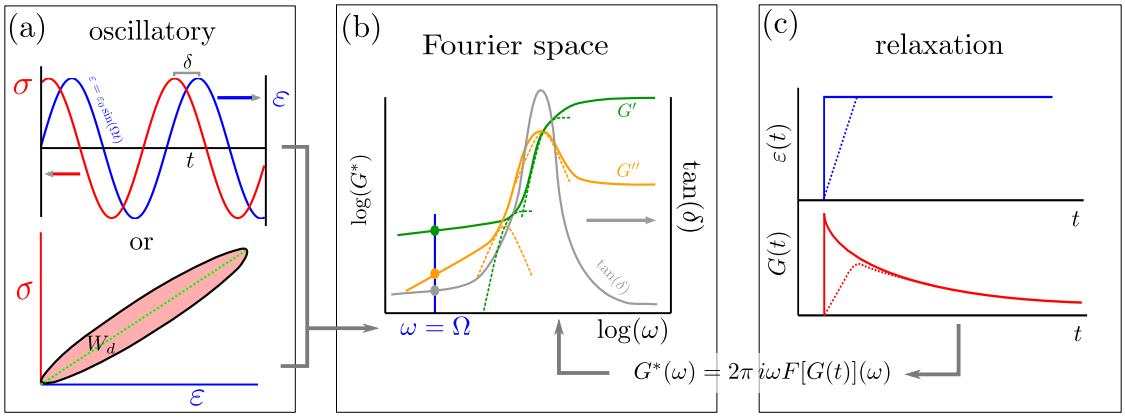

Figure 1: Overview over the connection between stress relaxation and oscillatory measurements and their relation to the complex modulus. (a) Sketch of two different methods to extract complex moduli at a defined frequency Ω from oscillatory measurements, see text. (b) Sketch of a typical viscoelastic master curve for filled rubber. The solid black line and dots indicate that the measurements form (a) sample a single frequency. The dashed lines exemplify Prony-elements fitted to the master curve. (c) Direct measurement of the relaxation kernel $G(t)$ by a stress relaxation experiment. The dashed line corresponds to non-infinite ("realistic") deformation speed, where relaxation starts during deformation.

2.3. Non-linear effects in (filled) rubber

Technical rubber usually contain nanoscopic particles to enhance and adjust its properties. At larger concentrations of common fillers (e.g. carbon black or silica) the filler network percolates and is able to transfer stress on its own. It is up to two orders of magnitude stiffer than the pure polymer matrix, but brittle and starts to break down at amplitudes of around 0.1 % strain. This softening, also called Payne effect (Hentschke, 2017), is non-linear and a major problem for technical analysis of rubber materials. An example is shown in Figure 2a (inset), where moduli obtained at 1 Hz are plotted vs. deformation amplitude. The symbols correspond to data extracted from the viscoelastic master curves. It can be shown PRONY that the curves with amplitudes above 0.1 % do not fulfill the Kramers-Kronig relations at relevant frequencies, such that the material cannot be considered linear anymore.

At larger strains the material continues to soften despite a fully broken filler network. This is called Mullins' effect and we refer the reader to Diani, Fayolle and Gilormini (2009); Plagge and Lang (2021) as a starting point. In this regime rubbery materials, when measured uniaxially, typically exhibit an S-shaped stress-strain curve and it seems clear that these materials cannot be linear elastic. However, under simple shear deformation the material's response appears to be linear up to strains often larger than 50 %. An example is shown in Figure 2b, where stress vs. strain for carbon black filled EPDM rubber is shown for different deformation modes. While uniaxial and equibiaxial deformation generate clearly non-linear curves the simple shear experiment (performed on a double sandwich geometry) is rather linear, if the clearly non-linear softening effect due to increasing strain levels is neglected. Looking at the inset we see that even an quasi-ellipsoidal shape is obtained (displacement is not sinusoidal but triangular, being responsible for the relatively "sharp edges"). However, intuition tells us that linearity is a material property which should not depend on the mode of deformation and in fact simple shear experiments performed on filled rubber at strains higher than about 0.1 % strain violate Kramers-Kronig relations (see above). Thus, the apparent linearity of (filled) rubbers at high strains under simple shear deformation has to be regarded as a mathematical coincidence[1]. The effect has repeatedly been labeled as "harmonic paradox" (Tolpekina et al., 2019; Lorenz, Pyckhout-Hintzen and Persson, 2014; Randall and Robertson, 2014).

2.4. Time-temperature superposition and mastering of rheological data

Mechanical measurements are limited in speed, because of device power, inertia effects and uncontrolled heat-builtup. Usually, reliable data on oscillatory rheometers can be obtained up to 100 Hz. Naturally, there is no lower boundary except of time. However, for scientific purposes and some practical correlations (e.g. predicting grip of rubbers used for tires), the material's response for a wider range of frequencies is required. Rubbers are essentially "entropic" materials, i.e. their mechanical response emerges from thermal fluctuations of the constituting polymer chains. Thus, if just one type (in a chemical sense) of polymers is used, the response can be traced back to the relaxation time of the primitive unit, that is a polymer segment[2]. It is helpful to imagine that the thermal motion of polymer chains "competes" with the external force: If we increase temperature, chains move faster and can faster adapt to an

[1] For the popular non-affine tube model of rubber elasticity (Klüppel and Schramm, 2000), which includes the "upturn" of stress visible in Figure 2 (uniaxial), it can be shown that under idealized simple shear conditions non-linearity in strain is a third order effect.

[2] Unfortunately, for this reason the whole concept breaks down for the large class of polymer blends, where two or more different polymers are mixed to achieve desirable properties.

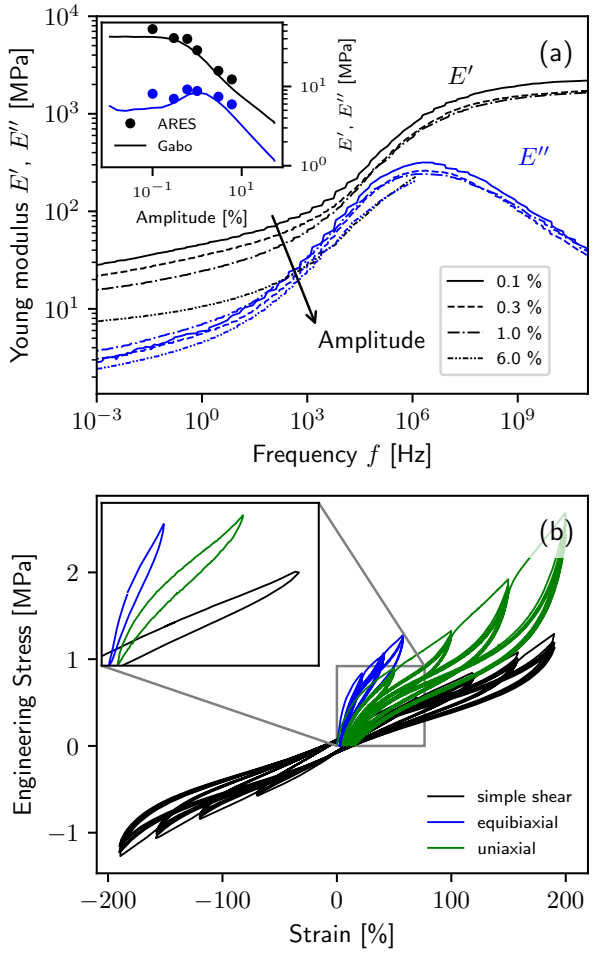

Figure 2: Tensile experiments on carbon black filled EPDM under different deformation modes with increasing strain levels. The inset shows the stable cycles of the first strain level.

external deformation. If we double both the chain movement speed and external deformation rate the resulting resistance towards deformation ("modulus") is the same. In other words: Just the ratio of thermal mobility and external (macroscopic) deformation rate determines G, or a low frequency measurement at low temperatures equals a high-frequency measurement at high temperatures. Mathematically, the material's response depends on ωa_T or t/a_T, where ω, a_T and t are frequency, a temperature dependent function and time, respectively. Thus, this so-called time-temperature superposition principle (TTSP) can be exploited to generate viscoelastic master curves over several decades of frequency. An example of real data obtained on sulfur cross-linked Ethylene-Propylene-Diene rubber (EPDM) filled with 50 phr reinforcing carbon black is shown in Figure 3a-c. For the lowest temperatures it can easily be seen that the individual measurements can be "stitched together" by horizontal shifting. As we're looking on a logarithmic frequency axis, this shifting corresponds to a multiplication in real space. For reasons becoming clear later it is best to do the shifting respective $\tan\delta$. The algorithm to construct a viscoelastic master curve is described in the following. It is implemented (using the shifting procedure described in Appendix A) to generate master curves automatically under www.plaggenet.de.

1. Select the measurement where shifting feels most reliable, e.g. by being smooth and exhibiting pronounced slopes that can be fit nicely to "neighboring" measurements. Usually, this is the case where $\tan\delta$ has a maximum (the corresponding temperature represents a rough estimate for the glass transition temperature T_g).

2. Shift all measurements together such that a continuous line is established. Pay attention: If the frequency axis is represented in log-scale (e.g. $\dots, 10^{-1}, 10^{1}, \dots$), then one has to multiply frequency with a_T to achieve a shift in the plot. If the decadic logarithm of the frequency data is plotted (e.g. $\dots, -1, 1, \dots$) one has to add/subtract the shift factor that is then called $\log_{10}(a_T)$. The result is presented in Figure 3d.

Two problems become apparent. (i) Shifting of noisy measurements, usually obtained at high temperatures, is not reliable (see inset of Figure 3d). (ii) Even though $\tan\delta$ appears reasonably smooth, there is some vertical offset in G' and G''. The latter is believed to originate from deviations of the TTSP due to the inclusion of filler. The latter introduces an energy-scale (physico-chemical bonds of filler-filler and filler-polymer) which violates the paradigm of a purely entropic material. Obviously, the data shown in Figure 3e can be converted to a continuous curve by vertical shifting. This corresponds to a multiplication of the modulus with a vertical shift factor b_T, i.e. $b_T G'$. If linear elasticity holds, G'' can be calculated from G' via Kramers-Kronig relations and it has to be multiplied with the same factor. The loss factor $\tan\delta$ is not affected by vertical shifting, because it cancels out:

$$\tan\delta(a_T\omega) = \frac{b_T G'(a_T\omega)}{b_T G''(a_T\omega)} \tag{36}$$

$$= \frac{G'(a_T\omega)}{G''(a_T\omega)} = \tan\delta(a_T\omega). \tag{37}$$

For this reason we shifted according to $\tan\delta$ in the first place.

3. Problem (i) of unreliable shift factors can be solved by fitting the Williams Landel Ferry (WLF) equation

$$\log_{10}(a_T) = -\frac{C_1(T - T_r)}{C_2 + (T - T_r)} \tag{38}$$

to the shift factors which seem to be reliable and extrapolating to the unreliable region. For a visual representation see next step.

4. Usually, one is interested in the frequency dependent response at a defined temperature, called reference temperature T_r, e.g. room temperature. As we have started the shifting respective a specific temperature,

we now have to adjust all shifting parameters such that a_T becomes one at T_r. In log-representation this is achieved by

$$\log_{10}(a_T) \rightarrow \log_{10}(a_T) - \log_{10}(a_{T_r}). \tag{39}$$

The adjusted logarithmic shift factors are shown in Figure 4a as symbols. Note that the latter is zero at $T_r = 20\,°\mathrm{C}$. The WLF Eq. (38) is presented as the solid blue line, fitted to the blue symbols, whose value is used for replacing the unreliable cross-marked shift factors[3]. In the example the parameters are $C_1 = 2.21$, $C2 = 95.6\,°\mathrm{C}$ and $T_r = 20\,°\mathrm{C}$. Afterwards, replot $\tan\delta$, G' and G''. The result for $\tan\delta$ is presented in Figure 3g. Compared with Figure 3d the frequency axis changed and there are minor differences in the zoomed region due to the extrapolation procedure. Subsequently, apply the shifting to G' and G'' (Figures 3e+f)

5. Problem (ii) is tackled by shifting vertically, starting with the newly chosen reference temperature. Usually, it is easier to perform vertical shifting on G', even though from a theoretical perspective it should work on G'' as well, if linear elasticity holds. For our example, the vertical shift factors $\log_{10}(b_T)$ are plotted in an Arrhenius representation (vs. $1/T$) in Figure 4b. In fact, the data is linear for high temperatures, supporting the hypothesis of an energy scale. The red line corresponds to a fit of the function

$$\log_{10}(b_T) = b_0 \mathrm{e}^{\frac{-E_b}{RT}} \tag{40}$$

with R being the universal gas constant and E_b some activation energy. After applying the vertical shift the master curves are complete. The result is shown in Figure 3g-i.

6. Finally, it is worth verifying that linear viscoelasticity holds. It is most probably violated, if

   - Vertical shift requires different b_T for G' and G'', or the shift factors obtained from one of the moduli does not generate a seemingly continuous curve for the other one.
   - Kramers-Kronig relations are not fulfilled. Probably the easiest way to check that is to fit a Prony-series (see the corresponding section). If G' and G'' cannot be fitted with the same set of parameters Kramers-Kronig is violated.

2.5. Transfer to FE-software, relaxation time spectrum and check for linearity

Finite-Element (FE) codes necessarily work in the time domain, such that, if linear viscoelasticity is employed, Eq. (1) is used. However, the evaluation of the whole hereditary integral is too costly to be performed on each time-step. This is circumvented by expressing Eq. (1) as a finite sum of elementary functions which can be computed as differential equations. The most simple and commonly used approach is

$$\dot{\sigma}_n = -\frac{\sigma_n}{\tau_n} + g_n \dot{\epsilon} \quad \text{for} \quad n = 1 \dots N \tag{41}$$

$$\text{with } \sigma = \sum_{n=1}^{N} \sigma_n \tag{42}$$

with relaxation times τ_n and weights g_n. If a visual representation is desired the differential equations can be understood in terms of a serial spring-damper system, also called Maxwell-Wiechert – elements. The differential equation (41) can be solved by standard methods (split of variables and integration). Its solution is, for each σ_n

$$\sigma_n(t) = g_n \int_{-\infty}^{t} G_{\tau_n}(t - t')\, \dot{\epsilon}(t')\, \mathrm{d}t' \tag{43}$$

with

$$G_{\tau_n} = \exp(-t/\tau_n)\theta(t). \tag{44}$$

The Heaviside function $\theta(t)$ ensures causality. Comparing Eq. (1) with Eqs. (43) and (41) we immediately conclude that our goal is to reproduce the relaxation function by

$$G(t) \simeq \sum_{n=1}^{N} g_n\, G_{\tau_n}(t) \tag{45}$$

Usually, a non-relaxing term is added (equivalent to $\tau \rightarrow \infty$) to the sum to ensure that the system stays a rigid body.

$$G(t) \simeq G_\infty + \sum_{n=1}^{N} g_n\, G_{\tau_n}(t) \tag{46}$$

We now have to find appropriate G_∞, g_n and τ_n to reproduce $G(t)$. As stated above the measurement of $G(t)$ in the time domain is often difficult. If we have obtained the complex modulus G^* we may simply exploit the equivalent Fourier transformed version of Eq. (44). Starting with Eq. (15)

$$G^*_{\tau_n}(\omega) = \sqrt{2\pi}\; i\omega\, \mathscr{F}\left[\mathrm{e}^{-t/\tau_n}\theta(t)\right](\omega) \tag{47}$$

$$= \frac{i\,\omega\tau_n}{1 + i\,\omega\,\tau_n} = \underbrace{\frac{\omega^2\tau_n^2}{1 + \omega^2\,\tau_n^2}}_{=:G'_{\tau_n}} + i\,\underbrace{\frac{\omega\tau_n}{1 + \omega^2\,\tau_n^2}}_{=:G''_{\tau_n}} \tag{48}$$

Thus, the goal is to express both the real and imaginary part of the experimentally found G^* by the following discrete

[3] We fitted the WLF equation before adjusting to T_r, because often the shifting factor a_{T_r} is already unreliable. Thus, we have to first get a reliable extrapolation to be able to do an accurate adjustment to T_r.

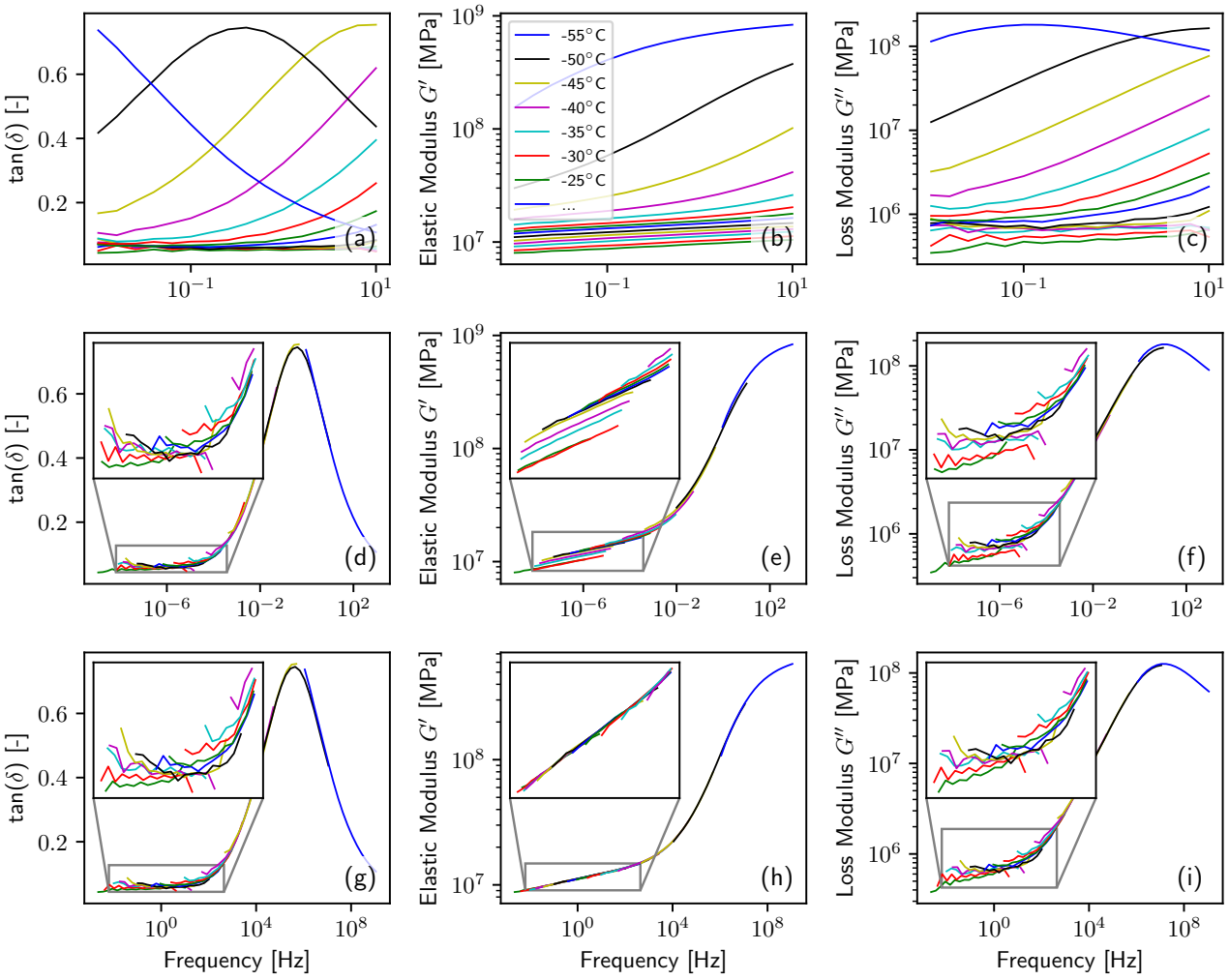

Figure 3: (a-c) Raw DMA data of carbon black filled EPDM at temperatures between -55 and 100 °C. (d-f) Same data, but shifted horizontally respective a reference temperature of −50 °C. The shift factors are shown in Figure 4a. (g-i) Same data, but horizontal shift factors refined by using the WLF equation, change of reference temperature to 20 °C and vertical shifting. The vertical shift factors are displayed in Figure 4b.

series[4]

$$G'(\omega) \simeq G_\infty + \sum_{n=1}^{N} g_n G'_{\tau_n} \tag{49}$$

$$\text{and } G''(\omega) \simeq \sum_{n=1}^{N} g_n G''_{\tau_n} \tag{50}$$

A schematic example is shown in Figure 1b, where the dashed lines correspond to two Maxwell elements, which approximate G^* in a certain frequency range.

[4]In fact, G' and G'' are not independent of each other. As $G(t)$ is a causal function, the Kramers Kronig relations hold. Checking the latter on numerical data is cumbersome, as the corresponding integrals have infinite boundaries which are experimentally not accessible and have to be extrapolated. However, Eq. (48) fulfills Kramers Kronig by construction and if G^* can be reproduced by a superposition of the latter according to Eqs. (49) and (50), then G^* obeys Kramers Kronig as well. If it cannot be reproduced like that the material probably behaves non-linear.

It turns out that it works best to optimize the logarithmic moduli, i.e. minimizing the functional

$$Err_G = \sum_{\omega_i} \Big[\Big(\log(G'_{\text{exp}}(\omega_i)) - \log(G'(\omega_i)) \Big)^2 \tag{51}$$

$$+ \Big(\log(G''_{\text{exp}}(\omega_i)) - \log(G''(\omega_i)) \Big)^2 \Big] \tag{52}$$

respective G_∞ and g_n, where the latter enter G' and G'' via Eqs. (49) and (50) and the ω_i denote the sampling points of the experimental data. The τ_n can be taken for optimization as well, but it is wise to set them fixed equidistant in log-space to avoid overparameterization and parameter correlations. Minimum and maximum τ can be determined from the range of frequencies, i.e $\tau_{\text{min}} = 1/f_{\text{max}}$ and $\tau_{\text{max}} = 1/f_{\text{min}}$. An example using some data also presented in Figure 2a is shown in Figure 5. In (a) the measurement with 0.1 % deformation amplitude is presented. A fit with 20 Prony

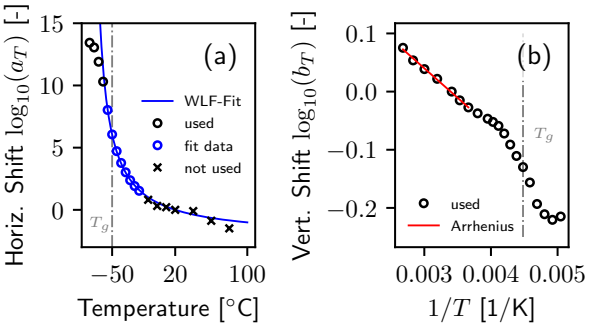

Figure 4: (a) Symbols denote horizontal shift factors obtained by algorithmic shifting. Black and blue circles are used in Figure 3. Blue circles are used for fitting the WLF-equation (solid line). Crossmarks are not used in Figure 3 and are replaced by VF-extrapolation. Grey line indicates an estimate for T_g. (b) Symbols originate from algorithmic shifting and are used in Figure 3. The red line shows a fit to Eq. (40).

elements (dashed line) is hardly visible, because it reproduces the experimental data almost exactly. This is proof that the material behaves linear viscoelastic. The corresponding relaxation time spectrum τ_n vs. g_n is shown in (c)[5]. Moreover, a fit with 10 Prony elements is shown, where the response of the individual element is still visible. As a rule of thumb, one Prony element per decade of frequency is required for a "smooth" fit. Figure 5b shows the same procedure for the 1.0 % measurement. Despite extensive tuning of the optimization algorithm a Prony series is unable to reproduce the experimental outcome. For this reason the material behaves most certainly not linear viscoelastic.

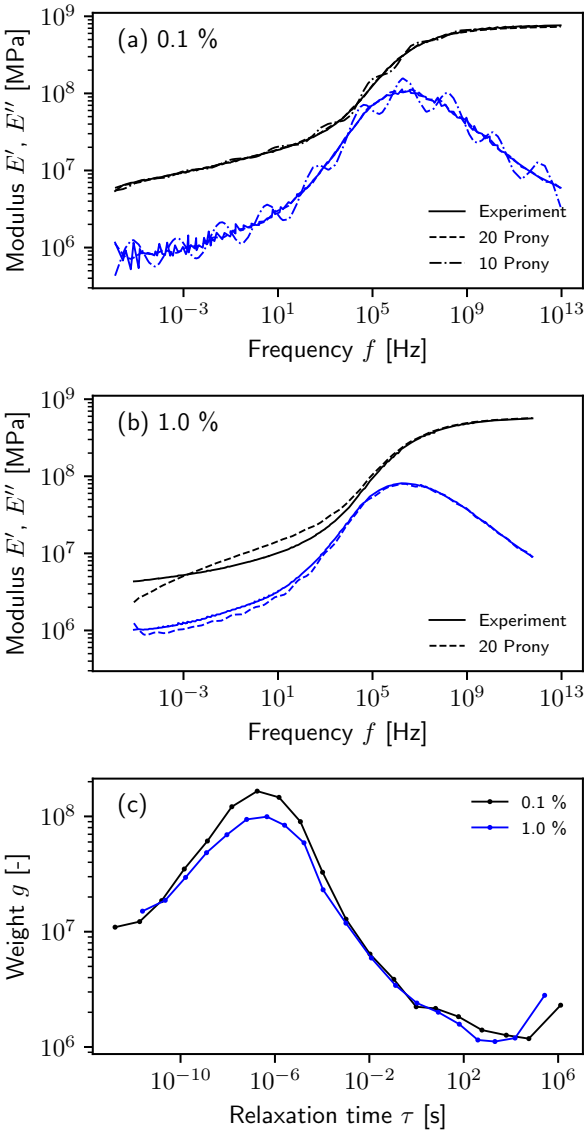

Figure 5: (a) Viscoelastic master curve at 0.1 % strain, taken from Figure 2a. Dashed line (hardly visible due to good fit) represents a fit of 20 Prony elements. The dashed-dotted line is a fit to 10 Prony elements. (b) Similar for the 1.0 % - measurement. The fit with 20 Prony elements does not converge, i.e. the material behaves non-linear. (c) Corresponding relaxation time spectra.

[5]Note that the relaxation time spectrum closely resembles the "mirrored" G''. This is not surprising, because G''_τ somehow resembles a δ-distribution (peaked) in log-space.

A. Algorithm for horizontal shifting

The shifting procedure described around Figure 3 can be done nicely by hand, but this requires much experience and time to be reproducible. A much better approach would be an algorithm that generates reproducible results. Such an algorithm is described in the following.

Let x_i and y_i be numerical sequences (measurement) of frequency and, say, $\tan\delta$ of the first signal. The latter shall be shifted (such that they "fit together") to the second sequence labeled by Y_i, correspondingly (frequency samples should be the same, i.e. $X_i = x_i \ \forall i$). It is important to note that these quantities should be calculated such that they fit the most appropriate representation, e.g. $x_i \simeq \log(f)$ and $y_i \simeq \tan\delta$. Abstracting the procedure carried out "by hand" we have to ensure two things: (i) Minimizing the cumulative distance in y direction between the two signals where both signals overlap after shifting[6], and (ii) maximizing overlap in x direction, because otherwise the obvious solution for (i) would be to shift such that there is minimal overlap and the cumulative distance is close to zero. Moreover, the data is sometimes wiggly and noisy and a human "shifter" would take that unconsciously into account by shifting to smoothed or interpolated curves. Thus, it is reasonable to express the numerical data as smoothed continuous curves $y(x)$ and $Y(x)$, respectively. Defining the shift in x as a it turns out that maximizing the functional

$$S(a) = \int_{\min(x_i)}^{\max(x_i)-a} \left(1 + \left(\frac{(y(x) - Y(x+a))}{\eta}\right)^2\right)^{-1} \mathrm{d}x \tag{53}$$

generates results close to the ones obtained by hand. The parameter η is used to tune the algorithm. Note that maximizing $S(a)$ ensures that both conditions are taken into account: (i) if the distance between $y(x)$ and $Y(x)$ becomes large, the integrand becomes vanishing and so does the functional (which is going to be maximized). (ii) If the distance is zero, the integral is just a measure of the overlap distance, i.e. $S(a) = \max(x_i) - a - \min(x_i)$ which is maximized for $a = 0$ (no shift). In practice, choosing $y(x)$ and $Y(x)$ to be fourth order polynomials of the experimental data has proven to work fine.

References

Diani, J., Fayolle, B., Gilormini, P., 2009. A review on the mullins effect. European Polymer Journal 45, 601–612.

Hentschke, R., 2017. The payne effect revisited. Express Polymer Letters 11.

Klüppel, M., Schramm, J., 2000. A generalized tube model of rubber elasticity and stress softening of filler reinforced elastomer systems. Macromolecular theory and simulations 9, 742–754.

Lorenz, B., Pyckhout-Hintzen, W., Persson, B., 2014. Master curve of viscoelastic solid: Using causality to determine the optimal shifting procedure, and to test the accuracy of measured data. Polymer 55, 565–571.

Plagge, J., Lang, A., 2021. Filler-polymer interaction investigated using graphitized carbon blacks: Another attempt to explain reinforcement. Polymer 218, 123513.

Randall, A.M., Robertson, C.G., 2014. Linear-nonlinear dichotomy of the rheological response of particle-filled polymers. Journal of applied polymer science 131.

Tolpekina, T., Pyckhout-Hintzen, W., Persson, B., 2019. Linear and nonlinear viscoelastic modulus of rubber. Lubricants 7, 22.

[6] If both measurements fit perfectly after shifting the y coordinates would be exactly the same